

Spatial Persistence of Angular Correlations in Amyloid Fibrils

Tuomas P. J. Knowles,^{1,2} Jeffrey F. Smith,^{1,2} Aidan Craig,¹ Christopher M. Dobson,^{1,3,*} and Mark E. Welland^{2,†}

¹Cavendish Laboratory, University of Cambridge, Cambridge CB3 OHE, United Kingdom

²Nanoscience Centre, University of Cambridge, Cambridge CB3 OFF, United Kingdom

³Department of Chemistry, University of Cambridge, Cambridge CB2 1EW, United Kingdom

(Received 8 February 2006; published 12 June 2006)

Using atomic force microscopy height maps, we resolve and quantify torsional fluctuations in one-dimensional amyloid fibril aggregates self-assembled from three different representative polypeptide systems. Furthermore, we show that angular correlation in these nanoscale structures is maintained over several microns, corresponding to many thousands of molecules along the fibril axis. We model disorder in the fibril in respect of both thermal fluctuations and structural defects, and determine quantitative values for the defect density, as well as the energy scales involved in the fundamental interactions stabilizing these generic structures.

DOI: 10.1103/PhysRevLett.96.238301

PACS numbers: 82.35.Pq, 87.14.Ee, 87.19.Xx

A crucial feature of living systems is the way newly synthesized polypeptide chains acquire a specific three-dimensional protein structure: an essential requirement for biological functionality [1]. However, it has become apparent that in addition to their normal native configuration, proteins can adopt an alternative highly organized state commonly known as an amyloid fibril [2]. These elongated nanoscale aggregates are composed of a number of intertwining protofilaments [2–5] and possess an ensemble of common chemical and structural properties, including the underlying “cross- β ” core structure. This consists of β strands separated by 4.8 Å along the fibril axis [6] held together by a dense hydrogen-bonding network thought to be the major contribution to the very high stability of the fibrils [2,7]. These structures can result from aberrations in the normal protein folding process and are hence involved in a range of human disorders, including Alzheimer’s disease and late onset diabetes [7]. However, the view is emerging that the amyloid state is a generic feature of polypeptides and accessible independently of their sequence [8], in strong contrast to the specific native states of proteins. In accordance with such a conclusion, a variety of phenomena in nature, including functional coatings of microorganisms [9] and the *in vivo* catalysis of polymerization reactions [10], have recently been shown to be associated with amyloid fibrils, suggesting the possibility of exploiting these structures for technological applications [11].

In this Letter we analyze by atomic force microscopy (AFM) the structure of amyloid fibrils on a mica surface with respect to torsional fluctuations along the helical fibril, and show that torsional correlations persist over microns and thus several thousands of β strands. Analysis based on a model including structural defects and thermal fluctuations enables us to determine the energy scales implicated in defects as well as in the interactions stabilizing the fibrils, making possible a quantitative understanding of some of the fundamental characteristics of these generic systems that underlie their pathogenic properties.

Data for this analysis were acquired by repeatedly passing the tip of an atomic force microscope (Molecular Imaging Pico Plus) in tapping mode over a suitable helical fibril, the fast axis of the scanner having been previously aligned with the fibril. In this study, we used two-filament fibrils from bovine insulin (51 residues, sample preparation as described in [5]) and four-filament fibrils from an 84 residue SH3 domain of PI3 kinase [4], which have been previously characterized [4,5] in terms of their protofilament structure by electron microscopy (EM) image reconstruction. These fibrils could readily be identified amongst other species present by comparing their height in AFM measurements with the dimensions of the EM electron density maps. Additionally, we considered fibrils from an 11 residue fragment 105–115 of transthyretin (TTR, experimental details as in [12]), which form well-defined helical morphologies, but for which no protofilament structure was available.

For a double helix, the topography displays height maxima [Fig. 1(a)] and minima separated by a twist angle of π . From the determination of the location of the extrema, the local twist angles along each fibril [Fig. 2(b)] can then be extracted. We now consider the average projection of two normal vectors following the twist separated by a fixed arc length. For an ideal helix, the projection oscillates between 1 and -1 for distances corresponding to even and odd integer numbers of periods, respectively. However, these maxima and minima in the projection are damped [inset of Fig. 2(b)] with increasing separation between the points, as the torsional correlation of the chain progressively decays. We measure the absolute values of the average projections, shown in Fig. 2(b), at integer multiples of the average period for each fibril in Fig. 2(a). The data are consistent with an exponential decay with correlation lengths of $3.7 \pm 0.1 \mu\text{m}$, $6.3 \pm 0.15 \mu\text{m}$, and $12.6 \pm 0.9 \mu\text{m}$ for the insulin, SH3, and TTR fibrils, respectively. These distances over which torsional correlations are maintained are quite remarkable for structures a few nanometers in diameter, and indicate a very high level of organization

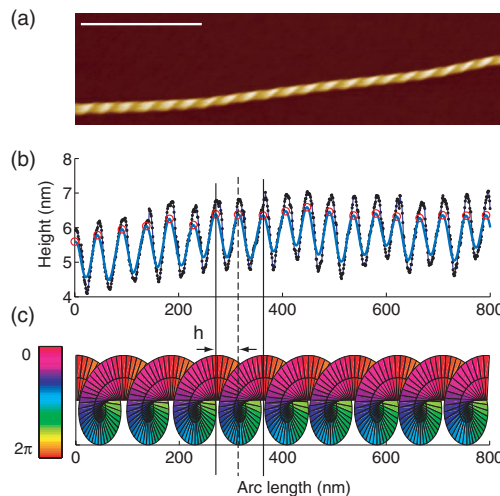


FIG. 1 (color online). (a) Topographic data were acquired in air in tapping mode for fibrils deposited on mica, shown here for a two-filament insulin fibril. Scale bar 250 nm. Because of tip-sample convolution effects, the distances in the sample plane are enlarged on the scale of the tip radius (7–10 nm), but height measurements are exact. (b) The height along the fibril backbone (small solid circles) was averaged over a window of 20 nm or twice the tip radius (blue/gray trace) and clearly displays maxima and minima (open circles) separated by a twist angle of π . From this height map, the local twist phase (c) can be extracted as described in the text.

within the core of the fibrils, despite the fact that a proportion of the protein outside the core can be unstructured [13]. Since the individual strands making up the fibril are separated by the generic spacing of 4.8 Å [6], the correlation lengths correspond to over 7700, 13 000, and 26 000 molecules along the fibril axis for the insulin, SH3, and TTR fibrils, respectively. We note that there is more variability in Fig. 2(a) in the twist between fibrils than within any one fibril; we suggest that this is an indication of the frustration in the underlying energy landscape, implying that there are several energetically close stable configurations for the peptides within the fibrils, and that successive elongation steps onto this template accurately follow the initial configuration. Such a conclusion is supported by the fact that we found no correlation between the twist and the position or orientation of the fibrils. This process is analogous to the recently proposed mechanism for the transmission of prion strains [14,15]. We can estimate the minimum number of stable configurations by considering the measured spread of 25%, 52%, and 19% for the mean fibril pitch for insulin, SH3, and TTR fibrils, which yields the approximate values 5, 10, and 4, respectively, since AFM distance measurements are precise to within better than 5%. This level of degeneracy is in very good agreement with the discovery [14] that there exist *in vivo* at least 8 prion strains defined by unique molecular conformations, and together with similar findings for Alzheimer's fibrils [16] suggests that this structural degeneracy is a generic characteristic of amyloid fibrils.

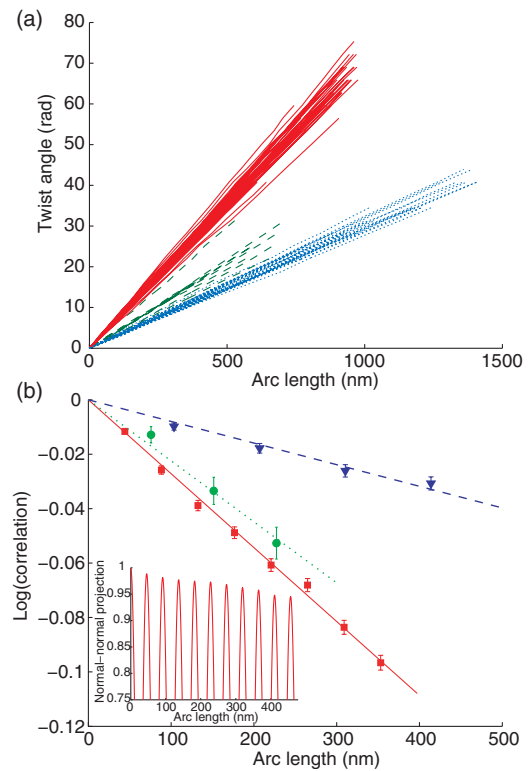


FIG. 2 (color online). (a) Cumulative twist angles measured for insulin (red solid lines), SH3 (green dashed lines), and TTR fibrils (blue dotted lines). (b) Logarithm of the average torsional correlation as a function of arc length measured at integer multiples of the period and one parameter fit to an exponential decay for insulin (red squares), SH3 (green circles), and TTR fibrils (blue triangles). Inset: Example of the damped oscillation of the absolute value of the normal-normal projection for an insulin fibril.

Two mechanisms contribute to the loss of angular order along the fibrils: thermal fluctuations and structural defects. To evaluate the role of thermal fluctuations, we consider the elastic Hamiltonian [17] for the twisting degree of freedom: $H[\varphi(s)] = \frac{C_T}{2} \int_0^l (\frac{\partial \varphi(s)}{\partial s})^2 ds - \omega_0^2 s^2$, where C_T is the torsional rigidity, $\varphi(s)$ is the measured local twist angle as a function of arc length s , and ω_0 is an intrinsic twist rate originating in chiral intermonomeric interactions [5]. The probability of observing a given twist angle difference Φ over some fixed length l for a fibril undergoing thermal fluctuations is given by the functional integral: $P_l(\Phi) = \frac{1}{Z} \int_{\varphi(s_0+l)-\varphi(s_0)=\Phi} \mathcal{D}[\varphi(s)] e^{-\beta H[\varphi(s)]} = \sqrt{\beta C_T / 2\pi l} e^{-(\beta C_T / 2l)(\Phi - \omega_0 l)^2}$, where $Z = \int \mathcal{D}[\varphi(s)] \times e^{-\beta H[\varphi(s)]}$ is the partition function and $\beta = (k_B T)^{-1}$ the inverse temperature. The probability for observing a defect with energy cost ϵ at any given interface between two molecules in the fibril is $p = \frac{1}{1+e^{\beta \epsilon}}$. If we assume that each defect introduces a random clockwise or anticlockwise change of $\pm \Phi_0$, the angle distribution converges as $N \gg 1$ to a normal distribution with variance $p\Phi_0^2 N$ (by the central limit theorem). We define $p/\lambda = \zeta$ as the one-dimensional defect density and $N\lambda = l$ as the arc length,

with λ the separation between molecules along the fibril axis. In our experiments we measure the sum of the contributions from thermal fluctuations and defects, therefore implying that the resulting probability distribution is the convolution of both distributions: $P_l(\Phi) = \sqrt{\beta C_T / 2\pi l} (\Phi_0^2 \zeta \beta C_T + 1) e^{-\beta C_T (\Phi - \omega_0 l)^2 / 2l(\Phi_0^2 \zeta \beta C_T + 1)}$. The oscillating mean normal-normal projection $\langle \cos(\Phi(l)) \rangle = \cos(\omega_0 l) e^{-l/2(\Phi_0^2 \zeta + 1/\beta C_T)}$ then is damped over the correlation length:

$$\xi = \frac{2}{\Phi_0^2 \zeta + \frac{1}{\beta C_T}}. \quad (1)$$

This result is the torsional analogue of the well-known exponential decay of the orientational correlation for bending degrees of freedom in semiflexible polymers [18] and has a clear connection to the theory of kinked semiflexible polymers [19].

We can now relate the experimental decay lengths measured for the three fibril systems to the prediction Eq. (1) of our model. We first note that for insulin fibrils, an independent estimate of the torsional rigidity $C'_T = 1.6 \pm 1.1 \times 10^{-26} \text{ N m}^2$ has been obtained by measuring the shear modulus from force spectroscopy [20]. This value of the torsional rigidity alone, without the contribution from structural defects, yields an expected correlation length of $\xi' = 2\beta C'_T = 7.8 \pm 5.5 \mu\text{m}$ [Eq. (1) with $\zeta = 0$]. This is of the same order of magnitude as the measurements here ($3.7 \mu\text{m}$), suggesting that the level of order is comparable to true crystalline structures of similar material properties and that the defect density in these systems is very low. We can now refine this idea by finding an upper bound for the defect density from the calculation of the number of defects required in the absence of thermal fluctuations to reproduce the experimental results.

Let us first consider purely entropic contributions ($p = 1$) by calculating the structural error $\Phi_0 = \sqrt{2\delta_\beta/\xi}$ allowed in the angular orientation of the individual β strands, by substituting $\zeta|_{p=1} = 1/\delta_\beta$ in Eq. (1) with $\delta_\beta = 4.8 \text{ \AA}$ the inter- β -strand spacing in amyloid fibrils, which is essentially sequence independent [6]. This gives values of Φ_0 of 0.9° , 0.7° , and 0.5° for the insulin, SH3, and TTR fibrils, respectively. Considering the fibril diameters d of 6.1 , 5.2 , and 10.8 nm , this implies that the atoms in the core structure have to be located within $\delta < \Phi_0 d/2 < 0.5 \text{ \AA}$ of their average position for the three fibril systems. Another way of interpreting the results to get an intuitive picture of the enthalpic effects is to substitute for Φ_0 the natural interstrand twist of 25° – 30° in globular proteins. This shows that a defect that changes the intrinsic interstrand twist rate of the fibril to that found in naturally occurring structures involves an energy cost of at least $\varepsilon = 6.9$, 7.5 , and $8.2k_B T$, for insulin, SH3, and TTR fibrils, respectively, values which are in the range of typical hydrogen bond energies at room temperature.

We finally examine the interactions between the individual protofilaments responsible for holding them together in the highly ordered helical fibril. Since the protofilaments have a finite bending rigidity C_B , there is an elastic energy cost $\Delta E_{\text{el}} = \int_0^l \frac{C_B \kappa^2(s)}{2} ds$ to bind them into helices of pitch $2h$ where they have to adopt a fixed curvature $\kappa = \frac{r}{r^2 + (h/\pi)^2}$. For the resulting structures to be stable, the elastic energy penalty has to be compensated by the energy gain from the attractive interactions. In order to quantify these energies, the bending rigidity of the individual insulin protofilaments of which the fibril is composed was estimated from measurements of ensemble averages of shape fluctuations from AFM topographic data of protofilaments adsorbed to a surface. Protofilaments for the analysis were identified by height as described in [21], and their dimensions ($3.1 \pm 0.4 \text{ nm}$) were in excellent agreement with the previous studies of the inner structure of insulin fibrils [5], implying that the free protofilaments are very similar to those incorporated into fibrils. The mean square distance $\langle u^2 \rangle$ from the center of a secant of length l connecting two points of the protofilament to the protofilament itself depends only on the bending rigidity C_B , and can be computed in two dimensions using the worm-like-chain model for semiflexible polymers [22,23] to yield $\langle u^2 \rangle = \frac{l^3}{48\beta C_B}$. The measurement of all combinations between the points on the fibril backbone, successively separated by the tip radius, over 185 insulin amyloid protofilaments (Fig. 3) reveals them to have a bending rigidity of $C_B = 1.9 \times 10^{-26} \text{ N m}^2$, which translates into a persistence length of $4.7 \mu\text{m}$.

So we can now place a lower bound $\varepsilon_{\text{att}} > \Delta E_{\text{el}}/s$ on the magnitude of the attractive interaction by using the values for the helical pitch $2h = 88.2 \text{ nm}$ and helix radius 1.6 nm determined from the AFM measurements, revealing that

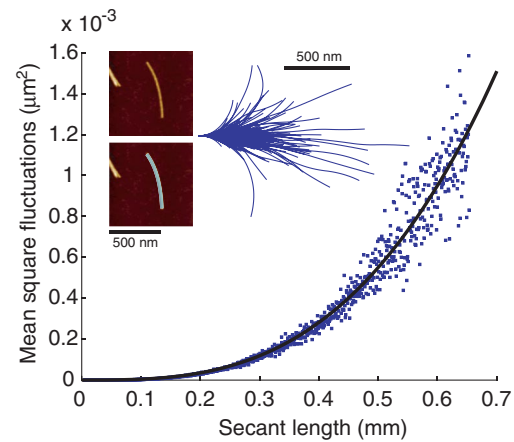


FIG. 3 (color online). The bending rigidity of insulin amyloid protofilaments, automatically traced from AFM topographs (inset), was estimated from the statistics of their shape fluctuations. Mean square fluctuations from the secant midpoint as a function of the secant length in 1000 bins, with a one parameter fit to a cubic equation describing the expected behavior for semiflexible chains.

there is an energy gain per unit length of at least $310k_B T/\mu\text{m}$ in the lateral association of two single insulin protofilaments into a mature fibril. To our knowledge, interaction energies of single protein filaments are known only for sickle hemoglobin fibers [24], yielding values ($4 \pm 3k_B T$) which are 2 orders of magnitude lower than our current measurements for amyloid fibrils. These comparisons between interactions involving proteins close to their native fold in sickle hemoglobin fibers and misfolded proteins in amyloid fibrils shed light on the driving forces of molecular evolution, and suggest that an extensive optimization of the fold of proteins is required to maintain the reversibility essential to functional biological systems and to avoid strong interactions that result in uncontrollable binding and potential toxicity. Furthermore, although the lateral attraction between protofilaments is an essential characteristic controlling the formation of amyloid structures, both *in vitro* and *in vivo*, very little is known about the molecular origins of these interactions. Our present results reveal that although the forces are still in the domain covered by dispersive and van der Waals interactions [25], the high level of order in the protofilament assembly suggests chemically specific and spatially localized interactions, which could, for example, take the form of hydrophobic packing.

These findings enable us to address a number of features associated with amyloid formation. It is known, for example, that although the amyloid state is accessible to many sequences, there is a strong preference for the incorporation of polypeptides of like rather than different sequences into individual fibrils [26]. This observation can now be understood in terms of the high level of local organization in the fibrils, which is disrupted at any interface between two different sequences in a single fibril, resulting in an energy penalty of several times the thermal energy as demonstrated here. We briefly discuss two further implications of our results. First, self-assembled nanostructures based on an amyloid core may find use in future applications due to their stability and mechanical rigidity. The degree of structural regularity down to the nanometer scale demonstrated here is likely to be vital in this context as it ensures that well-defined and uniform materials can be produced reliably, making possible a quantitative assessment of their suitability for different applications [11]. Second, in the light of the present results, it is clear that the high level of organization of amyloid fibrils contributes fundamentally to their stability, an essential feature of their involvement in disease [2,7], as the low defect density and strong interprotofilament interactions reduce the probability of their fracture and degradation by living systems.

We wish to thank Neil Birkett for providing the SH3 fibrils, and Cait MacPhee, Eugene Terentjev, Anthony Fitzpatrick, and Michele Vendruscolo for helpful discussions. T.P.J.K. acknowledges support from the IRC in Nanotechnology. C.M.D. acknowledges support from the Leverhulme Trust and Wellcome Trust.

*Electronic address: cmd44@cam.ac.uk

[†]Electronic address: mew10@cam.ac.uk

- [1] B. Alberts, A. Johnson, J. Lewis, M. Raff, K. Roberts, and P. Walter, *Molecular Biology of the Cell* (Garland, City, 2002), 4th ed.
- [2] C. M. Dobson, *Nature (London)* **426**, 884 (2003).
- [3] A. Aggeli, I. A. Nyrkova, M. Bell, R. Harding, L. Carrick, T. C. McLeish, A. N. Semenov, and N. Boden, *Proc. Natl. Acad. Sci. U.S.A.* **98**, 11857 (2001).
- [4] J. L. Jiménez, J. I. Guijarro, E. Orlova, J. Zurdo, C. M. Dobson, M. Sunde, and H. R. Saibil, *EMBO J.* **18**, 815 (1999).
- [5] J. L. Jiménez, E. J. Nettleton, M. Bouchard, C. V. Robinson, C. M. Dobson, and H. R. Saibil, *Proc. Natl. Acad. Sci. U.S.A.* **99**, 9196 (2002).
- [6] M. Sunde, L. C. Serpell, M. Bartlam, P. E. Fraser, M. B. Pepys, and C. C. Blake, *J. Mol. Biol.* **273**, 729 (1997).
- [7] M. B. Pepys, *Phil. Trans. R. Soc. B* **356**, 203 (2001).
- [8] M. Fändrich, M. A. Fletcher, and C. M. Dobson, *Nature (London)* **410**, 165 (2001).
- [9] M. R. Chapman, L. S. Robinson, J. S. Pinkner, R. Roth, J. Heuser, M. Hammar, S. Normark, and S. J. Hultgren, *Science* **295**, 851 (2002).
- [10] D. M. Fowler, A. V. Koulov, C. Alory-Jost, M. S. Marks, W. E. Balch, and J. W. Kelly, *PLoS Biol.* **4**, e6 (2006).
- [11] S. Zhang, *Nat. Biotechnol.* **21**, 1171 (2003).
- [12] C. P. Jaroniec, C. E. MacPhee, N. S. Astrof, C. M. Dobson, and R. G. Griffin, *Proc. Natl. Acad. Sci. U.S.A.* **99**, 16748 (2002).
- [13] M. Hoshino, H. Katou, Y. Hagihara, K. Hasegawa, H. Naiki, and Y. Goto, *Nat. Struct. Biol.* **9**, 332 (2002).
- [14] J. Safar, H. Wille, V. Itri, D. Groth, H. Serban, M. Torchia, F. E. Cohen, and S. B. Prusiner, *Nat. Med. (NY)* **4**, 1157 (1998).
- [15] M. Tanaka, P. Chien, K. Yonekura, and J. S. Weissman, *Cell* **121**, 49 (2005).
- [16] A. T. Petkova, R. D. Leapman, Z. Guo, W.-M. Yau, M. P. Mattson, and R. Tycko, *Science* **307**, 262 (2005).
- [17] A. M. Kosevich, E. M. Lifshitz, L. D. Landau, and L. P. Pitaevskii, *Theory of Elasticity* (Butterworth-Heinemann, Washington, DC, 1986).
- [18] M. Doi and S. F. Edwards, *The Theory of Polymer Dynamics* (Oxford University Press, Oxford, 1986).
- [19] P. A. Wiggins, R. Phillips, and P. C. Nelson, *Phys. Rev. E* **71**, 021909 (2005).
- [20] J. F. Smith, T. P. J. Knowles, C. E. MacPhee, C. M. Dobson, and M. E. Welland (to be published).
- [21] C. Ionescu-Zanetti, R. Khurana, J. R. Gillespie, J. S. Petrick, L. C. Trabachino, L. J. Minert, S. A. Carter, and A. L. Fink, *Proc. Natl. Acad. Sci. U.S.A.* **96**, 13175 (1999).
- [22] E. M. Lifshitz and L. D. Landau, *Statistical Physics* (Butterworth-Heinemann, Washington, DC, 1984).
- [23] J. C. Wang, M. S. Turner, G. Agarwal, S. Kwong, R. Josephs, F. A. Ferrone, and R. W. Briehl, *J. Mol. Biol.* **315**, 601 (2002).
- [24] C. W. Jones, J. C. Wang, R. W. Briehl, and M. S. Turner, *Biophys. J.* **88**, 2433 (2005).
- [25] C. W. Jones, J. C. Wang, F. A. Ferrone, R. W. Briehl, and M. S. Turner, *Faraday Discuss.* **123**, 221 (2003).
- [26] C. F. Wright, S. A. Teichmann, J. Clarke, and C. M. Dobson, *Nature (London)* **438**, 878 (2005).